ISBN: 978-981-18-5852-9
WCSE 2022 Spring Event: 2022 9th International Conference on Industrial Engineering and Applications
doi: 10.18178/wcse.2022.04.024

Design of Rehabilitation Protective Gear for Distal Radius Fracture

Jia-bao Guo [1], Gang Chen [1+] , Xing-song Wang[1] and Meng-qian Tian[1]

[1] College of Mechanical Engineering, Southeast University

Abstract. Distal radius fracture is the most common fracture type of upper limbs. After manual reduction, the affected part should be fixed mainly, and proper rehabilitation training should be done according to the healing situation to reduce the occurrence of complications. At present, the commonly used fixation methods include plaster, small splint, polymer bandage, etc. They all have their defects and cannot meet the training needs of patients in the early stage of rehabilitation. Therefore, this paper proposes a rehabilitation protective gear for distal radius fracture based on reverse modeling. The protective gear is divided into four parts: palm module, forearm module, palm flexion-dorsiflexion locking module, and radial-ulnar deviation locking module. Firstly, the structure of these modules is designed, in which 3D scanning technology is used in the forearm module to collect data of volunteers' upper limbs for reverse modeling. Secondly, ANSYS Workbench is used to do finite element analysis of the protective gear. The results show that the protective gear can satisfy the needs of external fixation of the affected part. After that, the lightweight design of the forearm module is carried in Rhino Grasshopper. The finite element analysis results show that the weight of the optimized forearm module is reduced to 86% of the original one while ensuring the mechanical properties. Finally, it is verified by experiments that the motion range of the protective gear can meet the needs of patients for early rehabilitation training.

Keywords: 3D reconstruction, protective gear, distal radius fracture.

1. Introduction

Distal radius fracture is the most common fracture type of upper limbs, accounting for about 1/10-1/6 of all fracture types [1]. It often occurs in two groups of people: one is adolescent group, which is mostly manifested as “high energy” fracture caused by car accidents, falling from high altitude and other factors; The other is the middle-aged and elderly population, which is often accompanied by loose fracture and manifested as “low energy” fracture [2-3]. At present, conservative treatment and surgical treatment can be used for distal radius fractures. Compared with surgical treatment, conservative treatment is performed by doctors by manual reduction, which is not only low in treatment cost but also simple in operation [4], so it is more easily accepted by patients.

In the process of conservative treatment of distal radius fractures, the affected part often needs external fixator braking for a period of time to achieve clinical healing. At present, plaster, small splint, and polymer bandage are often used as external fixation equipment [5]. However, all three kinds of fixators have limitations: plaster fixation is heavy and air permeability is poor; If small splint fixation is not used properly, it is easy to compress the patient's osteofascial and cause osteofascial syndrome; Polymer bandages have poor plasticity.

At the same time, in the process of rehabilitation of distal radius fractures, timely specific rehabilitation training at the corresponding stage of fracture healing is beneficial to the recovery of injured soft tissue muscle strength and also helps to reduce joint movement restrictions caused by fixation. Orthopedic rehabilitation divides fracture recovery into three stages: protection period, stable period, and healing period. In the first two stages, the braking protection of the fixator is the main one, and moderate radiocarpal joint movement should be carried out according to the healing situation. During the healing period, impedance training can be performed to restore muscle strength. If rehabilitation training is not paid enough attention in the first two stages, a series of static splints can only be used to passively improve joint stiffness and limited joint movement in the healing stage. However, it is not easy to complete rehabilitation training by the aforementioned methods.

+ Corresponding author. Tel.: + 86 13601461145.
E-mail address: ldd1485@163.com.

E-mail address: ldd1485@163.com.

Many researchers use 3D printing fixators to improve the limitations of the above three fixation devices. Filip Górski [6] chose the combination of ABS and TPU to improve the comfort of the fixator. Huhn Kim [7] divided the fixator into inner and outer parts, which increased the air permeability of the fixator. Hui Lin et al. [8] and Pasquale Guida et al. [9] added an opening gap on the printout to adapt to limb swelling during treatment. In addition, many scholars have researched in the direction of upper limb rehabilitation equipment. J. Beekhuis et al. [10] reduce the discomfort of the wearer during training by increasing the freedom of rehabilitation institutions. Lin-cong Luo et al. [11] designed desktop wrist rehabilitation equipment controlled by a motor. However, the above research is either bulky or can not meet the rehabilitation training needs of patients. Patients with distal radius fractures have the ability to move autonomously and do not need a booster. But there are relatively few devices that can provide fixation for patients when they need braking protection and do not hinder their movement when they need rehabilitation training.

Given the above situation, for patients with distal radius fractures, this paper puts forward a light and breathable external fixation protective gear, which can meet the needs of patients' independent training during fracture protection and stability stages.

2. Overall Structural Design

2.1. Analysis of movement form and range of wrist joint

The wrist joint is a typical elliptical joint, which can do volar dorsal rotation and radial ulnar rotation, which are called palmar flexion, dorsal extension, radial deviation and ulnar deviation respectively. The motion in two directions can be combined to form a circular motion. The range of motion of the wrist joint can be divided into the normal range of motion and the functional range of motion. The former is the one allowed by anatomy, while the later is the one that can meet the needs of people's daily life. For rehabilitation after fracture, the protective gear to be designed should meet the functional range of wrist motion. If the hand and forearm are naturally straightened in a line, and the palm is recorded as the 0 positions of the wrist joint, the design objectives of the wrist joint are shown in Table 1 .

Table 1: Motion form and range of wrist joint

Modes of movement	Normal range of motion	Functional range of motion	Design objective
Palmar flexion	75°	15°	30°
Dorsal extension	70°	30°	60°
Radial deviation	20°	10°	15°
Ulnar deviation	35°	15°	20°

2.2. The overall structure of the protective gear

As shown in Fig.1, the external fixation rehabilitation protective gear is mainly composed of a palm module, radial-ulnar locking mechanism, palm flexion-dorsiflexion locking mechanism, and forearm module. Among them, the shape and size of the forearm module are greatly affected by individual differences of patients, so this part adopts reverse modeling technology to realize personalized customization. The degree of muscle development of the palm part is similar, with little difference in shape and obvious difference in size. Therefore, after completing a group of designs, different sizes of palm models can be designed according to the human body size standard. In this design, the palm module and forearm module are fixed with a hook and loop, which can be adjusted tightly according to the swelling degree of the affected part.

Radial-ulnar locking mechanism and palm flexion-dorsiflexion locking mechanism are the connecting parts of the palm and forearm module, which can limit the movement in two directions and realize the external fixation of the affected part at the initial stage of fracture. As shown in Fig.2(a), by tightening the plum handle to engage the mating teeth, palm flexion-dorsiflexion locking mechanism and the forearm module are engaged through the hexagonal hole and slot. After locking, there is no relative movement between the palm module and the forearm module. Since the distance between two adjacent teeth in the locking module is 10 degrees, the user can keep a fixed posture at any 10 degrees within the maximum range of movement in the direction. As shown in Fig.2 (b), the radial-ulnar locking module uses pins to achieve motion locking in this direction. After the pin enters the hole, the limiting block can prevent the pin from falling off and realize the stable fixation in this direction. There is a limit hole every 5 degrees in the radial/ulnar deviation direction, so locking can be realized at any 5 degrees within the maximum range of motion in this direction.

The torques produced by wrist joint movement in palmar flexion/dorsiflexion and radial/ulnar deviation directions are 2Nm respectively, and the designed protective gear needs to keep effective fixation under the above torque conditions. And because the surface of protective gear is mostly irregular, except bolts, pins, plum handles, etc., the rest are processed and manufactured by 3D printing. After comparative analysis, photosensitive resin is selected as printing material, and its mechanical properties are shown in Table 2.

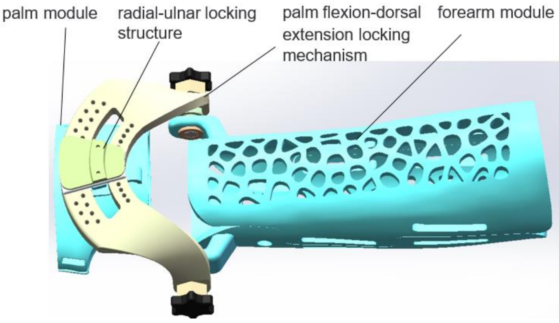

Fig. 1: Overall mechanism of the protective gear.

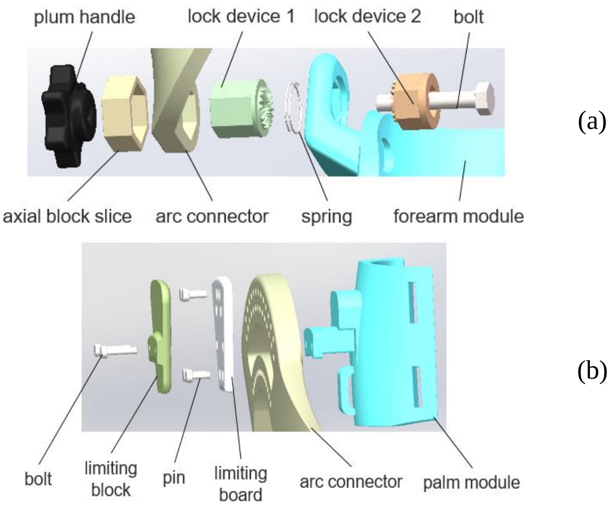

Fig. 2: (a) Palm flexion-dorsal extension locking mechanism
(b) Radial-ulnar locking structure.

Table 2: Mechanical properties of 3d printing materials

Mechanical properties	Numerical value
Density (g/cm^3)	1.15
Tensile modulus (MPa)	2600
Bending modulus (MPa)	2700
Poisson's ratio	0.42

2.3. Reverse modeling of forearm module

To make the protective gear fit the shape size of the forearm better, the reverse modeling of the forearm module is carried out in this paper, that is, collect the point cloud data of the forearm to get a three-dimensional model, and complete the design on the obtained model. There are usually three ways to obtain human body surface data: computed tomography (CT), magnetic resonance imaging (MRI), and three-dimensional scanning. Because the three-dimensional scanner is easy to obtain and operate, this paper uses it to scan the arm. The specific operation process is as follows: the experimenter holds a three-dimensional scanner to rotate and collect the point cloud data of volunteers' forearm at a speed of 3 minutes per circle; Import the collected data into MeshLab for point cloud splicing, noise reduction, filling, etc., and get a complete forearm triangular patch model; Using Rhinoceros software to intercept the required data and generating multiple surfaces; Finally, in SolidWorks, the placement of the hook and loop is designed to make the tightness of the protective gear easy to adjust. The process is shown in Fig.3.

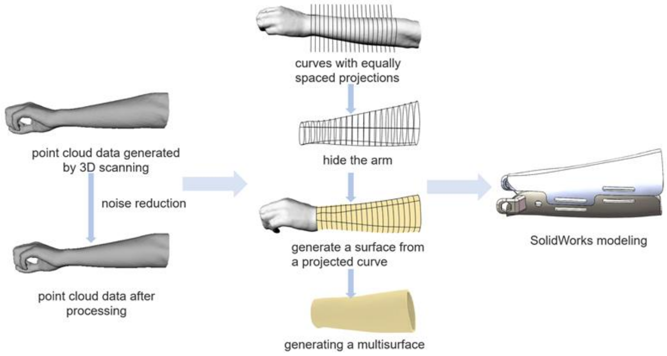

Fig. 3: Flow chart of reverse modeling.

3. Strength Analysis and Lightweight Design

3.1. Finite element analysis of protective gear

At the initial stage of rehabilitation, protective gear should ensure good fixation of the affected part[12]. The torques produced by wrist joint motion in palmar flexion/dorsiflexion and radial/ulnar deviation direction is 2Nm respectively. For the sake of safety, this paper verifies the deformation and stress nephogram of the protective gear under the action of 2.5 Nm torque in the above two directions and then judges the fixing effect of the protective gear.

Because fastening bolts, pins, etc. are different from the main materials of protective gear, and the strength of 3D printing materials is relatively low, the stress effect of 3D printing parts is mainly considered in the analysis. As can be seen from Fig.4, the maximum equivalent stress of the protective gear under the action of external force is 31.85 Mpa, which appears on the meshing teeth in the palm flexion-dorsiflexion locking structure. This is consistent with the actual situation. In addition, the maximum equivalent stress of the forearm is 13.24 Mpa, which appears at the connection part of the forearm module. Considering the actual situation, when the protective gear is in a fixed state, the stress of this part is easy to increase under the action of external load. However, on the whole, the equivalent stress of the forearm module is far lower than the tensile strength of 60Mpa, so there is room for optimization in the forearm module. From the analysis of deformation, the maximum deformation of protective gear appears on the palm module, and the deformation is 1.68 mm. Considering the actual situation, the farther the distance between a point on the palm module and the center axis of rotation, the greater the displacement, so it is relatively reasonable that the maximum deformation of the protective gear appears at the edge of the palm module. Slight movement of fracture end can promote fracture healing, and because muscle tissue is elastic, the movement of fracture end caused by hand displacement less than 2 mm is very small, so it can meet the needs of fixation.

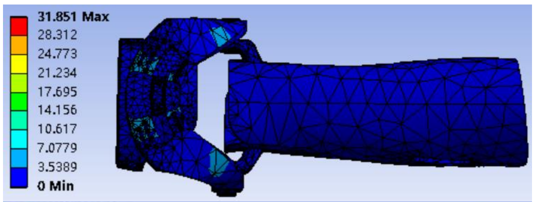

(a)

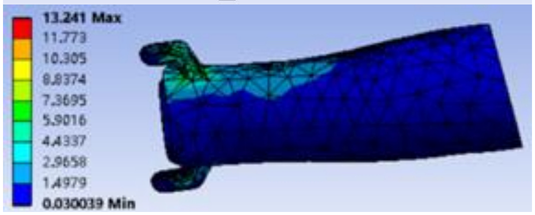

(b)

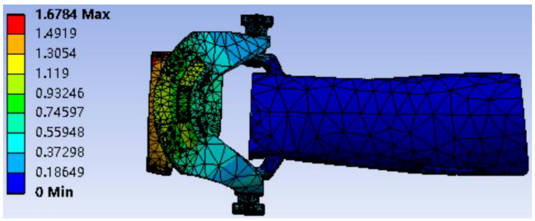

(c)

Fig. 4: (a) Equivalent stress nephogram of whole module
(b) Equivalent stress nephogram of forearm module
(c) Equivalent deformation of whole module.

3.2. Lightweight design of forearm module

As the main part of protective gear, the lightweight design of the forearm module is of great significance to reduce 3D printing time and increase the air permeability of protective gear. Generally speaking, there are two ways to realize lightweight design: one is to use lightweight materials, and the other is to choose appropriate structures, such as commonly used sandwich structures, hollow structures, and three-dimensional lattice structures. Because the protective gear itself is processed by 3D printing, the choice of materials is limited under the condition of ensuring mechanical properties, and considering the irregularity of the protective gear itself, this paper adopts the hollow structure to the lightweight design of the protective gear.

Tyson polygon is a commonly used method to build an irregular honeycomb model. The basic idea is to generate a series of random points in the hollow plane, and the distance from all points in the unit area of each Tyson polygon to the unit seed is closer than that from them to other unit seed points. In this paper, Tyson Polygon and Rhino Grasshopper are used to hollow out the protective gear. The basic process is shown in Fig.5. After the Voronoi partition is completed, every generated Tyson polygon area is scaled, each reduced unit is the actual hollow position, and other connected areas are reserved parts. The generated two-dimensional Tyson polygon can be attached to the surface that needs to be hollowed out. In this paper, the scaling ratio of Voronoi is 0.7, and 120 hollow points are distributed on the upper and lower surfaces. The effect of the obtained model after assembly in SolidWorks is shown in Fig.6.

Using the same load and boundary conditions mentioned above, the finite element analysis of the hollowed-out protective gear model is carried out, and the equivalent stress and equivalent strain results are shown in Fig.7. It can be seen from the figure that the maximum deformation of the protective gear model is 1.68 mm, which is not much different from the original model. The maximum equivalent stress of the optimized model is 32.19 Mpa, and the maximum equivalent stress of the forearm is 13.52 Mpa, which is slightly increased compared with the original model. The mass of the forearm module is reduced from 163g to 140g after optimization, which is equivalent to 86% of the original model. Compared with the original model, the air permeability is greatly improved.

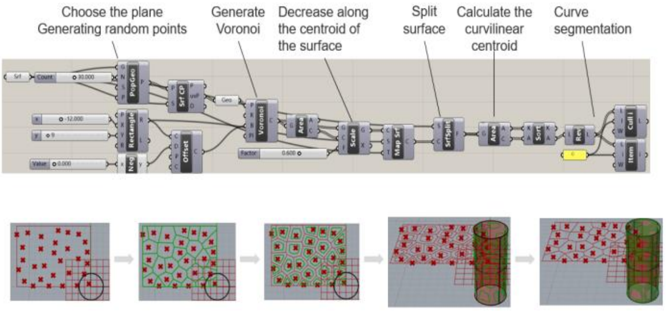

Fig. 5: Forearm module hollow flow chart.

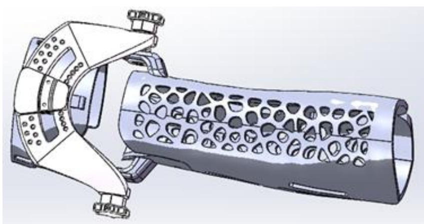

Fig. 6: Hollow-out protective gear.

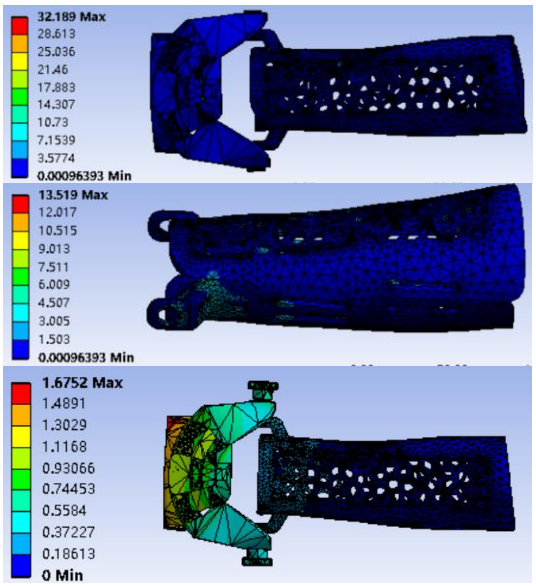

(a)

(b)

(c)

Fig. 7: (a) Equivalent stress nephogram of whole module
(b) Equivalent stress nephogram of forearm module
(c) Equivalent deformation of whole module.

4. Experiments

The external fixation protector has two states: fixation and movement. It can brake the affected part in the fixed state, which has been theoretically verified in the finite element analysis of protective gear, so it will not be repeated here. The rehabilitation process of distal radius fracture can be divided into three stages: protection period, stable period and healing period. In the first two stages, the braking protection of the fixator is the main one, and moderate radiocarpal joint movement should be carried out according to the healing situation to avoid joint stiffness. For example, during the protection period, palmar flexion, dorsal extension, radial deviation and ulnar deviation can be gently done according to fracture healing situation. In the stable period, it is very important to recover the range of motion of wrist joint. It is better for patients to do the above movement to achieve the functional range of motion of wrist joint. Therefore, the range of motion of the external fixation protector should be greater than the functional range of motion of the wrist joint which is shown in Table 1.

In order to verify the range of motion that external fixation protective gear can achieve in the early rehabilitation training. In this paper, a model is printed in 3D, and an attitude sensor is installed on the hand module. The actual motion range of the model is judged by the data which returned from the attitude sensor. As shown in Fig.8, besides attitude sensors, the physical model also reserves placement positions for other sensors. After wearing the external fixation protective gear, volunteers performed palm flexion-dorsiflexion, and ulnar-radial deviation. During the experiment, we collected about 1900 points in each direction to draw the actual motion curve, as shown in Fig.9. It can be seen from the curve that after wearing the protective gear, the range of motion in radial deviation and ulnar deviation is over 20°, the range of motion in palm flexion direction can reach nearly 40°, and the range of motion in dorsiflexion direction can reach about 70°. The range of motion in each direction can cover the requirements in the design goal.

(a)

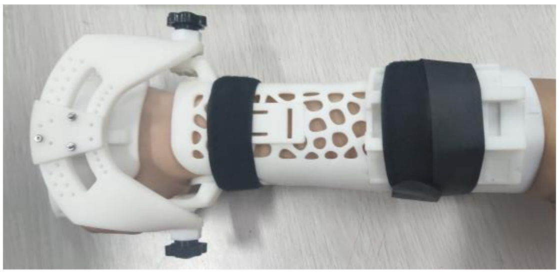

(b)

Fig. 8: (a) The attitude sensor is placed on the hand module
(b) Volunteers wear physical models.

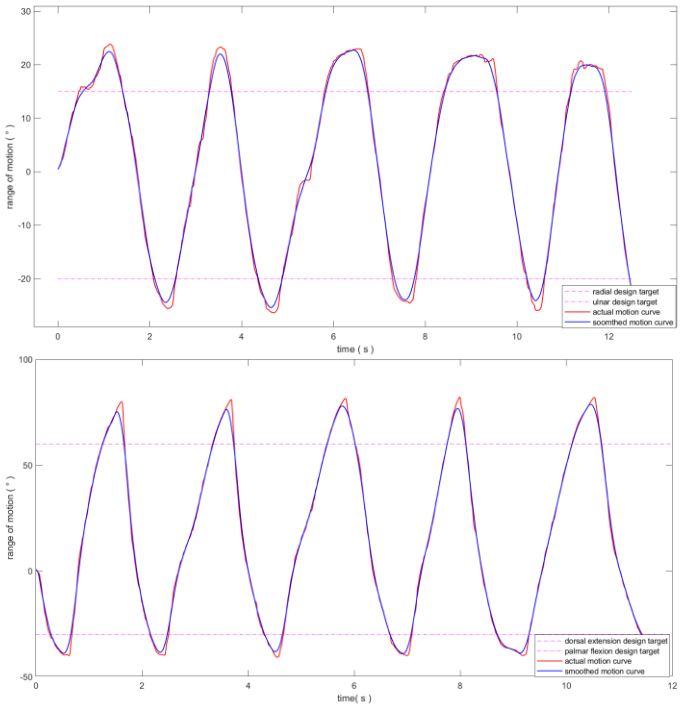

(a)

(b)

Fig. 9: (a) Motion curve of radial-ulnar deviation direction and design goal
(b)Motion curve of palm flexion-dorsiflexion direction and design goal.

5. Conclusions

In this study, a new type of external fixation protector for distal radius fractures was proposed, and its lightweight design was carried out. Using 3D scanning, 3D printing, and other technologies, the protective gear can better fit the patient's body surface, improve the defects of traditional fixing methods, and realize personalized customization. At the same time, the protective gear can switch between fixed and movable states, so as to meet the needs of patients for early fixation of affected parts and rehabilitation training. The results of finite element analysis show that the protective gear can ensure good fixing effect. At the same time, the experiment shows that the actual motion range of the protective gear can cover the functional mobility of the wrist. However, compared with the traditional fixed method, 3D printing fixator takes longer time. How to reduce the 3D printing time are the problems that need to be considered in the future of this study.

6. Acknowledgements

The author would like to thank the orthopaedic physician team of Nanjing First Hospital for their help, and we would also like to express our sincere gratitude to the anonymous reviewers for their valuable comments, which have greatly improved this article.

7. References

[1] C. S. Wang, Q. G. Wang, “Fracture of distal radius,” *Journal of Geriatrics and Healthcare*, vol. 13, no. 6, pp.

383-390, 2007.

[2] M. Leixnering, R. Rosenauer, C. Pezzei, J. Jurkowitsch, T. Beer and T. Keuchel, “Indications surgical approach reduction and stabilization techniques of distal radius fractures,” *Journal of Archives of Orthopaedic and Trauma Surgery,* vol. 140, no. 5, pp. 611-621, 2020.

[3] C. Jantzen, L. K. Cieslak, A. F. Barzanji, P. B. Johansen and S. W. Rasmussen, “Colles' fractures and osteoporosis--A new role for the emergency department,” *Journal of Injury,* vol. 47, no. 4, pp. 930-933, 2015.

[4] Z. H. Bai, “Application of 3D printing in treatment and rehabilitation of distal radius fracture,” *Journal of Development and Innovation of Mechanical and Electrical Products,* vol. 34, no. 2, pp. 37-39, 2021.

[5] L. Lu, Y. Yu, “Study on 3D printing phalangeal fracture brace,” *Journal of Aerospace Medicine and Medical Engineering,* vol. 30, no. 4, pp. 263-265, 2017.

[6] [6]F. Górski, W. Kuczko, W. Weise and R. Wichniarek, “Prototyping of an individualized multi-material wrist orthosis using fused deposition modelling,” *Journal of Advances in Science and Technology – Research Journal,* vol. 13,no. 4, pp. 39-47, 2019.

[7] K. Huhn, J. Seongwon, “Case study: Hybrid model for the customized wrist orthosis using 3D printing,” *Journal of Mechanical Science and Technology,* vol. 29, no. 12, pp. 5151-5156, 2015.

[8] H. Lin, L. Shi and D. Wang, “A rapid and intelligent designing technique for patient-specific and 3D-printed orthopedic cast,” *Journal of 3D Printing in Medicine,* vol. 2, no. 1, pp. 2-10, 2016.

[9] P. Guida, A. Casabur, T. Busiello, “An alternative to plaster cast treatment in a pediatric trauma center using the CAD/CAM technology to manufacture customized three-dimensional-printed orthoses in a totally hospital context: a feasibility study,” *Journal of Wolters Kluwer Health,* vol. 28, no. 3, pp. 248-255, 2019.

[10] J. H. Beekhuis, A. J. Westerveld, H. van der Kooij and A. H. A. Stienen, “Design of a self-aligning 3-DOF actuated exoskeleton for diagnosis and training of wrist and forearm after stroke,” *2013 IEEE 13th International Conference on Rehabilitation Robotics (ICORR),* Seattle, WA, USA, 2013, pp. 1-5.

[11] L. Luo, L. Peng, Z. Hou and W. Wang, “Design and control of a 3-DOF rehabilitation robot for forearm and wrist,” *2017 39th Annual International Conference of the IEEE Engineering in Medicine and Biology Society (EMBC),* 2017, pp. 4127-4130.

[12] I. Panagopoulos, P. Katrakazas, and D. Koutsouris, “Design and development of an airborne biomedical signal device for urgent care situations,” *International Journal of Electronics and Electrical Engineering,* Vol. 8, No. 2, pp. 31-35, June 2020. doi: 10.18178/ijeee.8.2.31-35